Characterizing Spatiotemporal Variation in Leaf Area Index of Pine Plantations across Virginia

Wyatt C. McCurdy

Thesis submitted to the faculty of the Virginia Polytechnic Institute and State University in partial fulfillment of the requirements for the degree of

Master of Science
In
Forestry

R. Quinn Thomas
Valerie A. Thomas
Randolph H. Wynne

December 2, 2019
Blacksburg, VA

Keywords: Remote Sensing; Landsat; Simple Ratio Index; Leaf Area Index; Loblolly Pine

Characterizing spatiotemporal variation in leaf area index of pine plantations across Virginia

Wyatt C. McCurdy

ABSTRACT

Loblolly pine is an important managed tree species within the southeastern United States, and better understanding spatial patterns in its productivity has potential to contribute to both modeling and management of the species. Using recently-created pine management maps specific to Virginia and empirical relationships predicting pine LAI from the Landsat satellite, we conducted a statewide analysis of temporal patterns in stand-level southern pine leaf area index (LAI) following clear-cut and planting. Here, using 28 years of Landsat time-series data for 13,140 stands that were clear-cut between 2014-2017, we examined 1) when LAI peaked over the rotation, and 2) how LAI in each stand compared to a recommended fertilization threshold of 3.5 LAI. We found that, on average, winter LAI reached a maximum of 2.02., which can be approximately doubled to give a summer LAI of 4.04, and within stand peak occurred between years 13 and 15. We also found that around 45.8% of stands achieved an LAI value higher than 3.5: a fertilization threshold recommended for managed stands in Virginia. The dataset produced by our analysis will bolster information required for modeling loblolly pines as a plant functional type in regional land simulations, and the finding that most stands are below the recommended LAI fertilization threshold will fuel further management-motivated research.

Characterizing spatiotemporal variation in leaf area index of pine plantations across Virginia

Wyatt C. McCurdy

GENERAL AUDIENCE ABSTRACT

Management of pines in the southeastern U.S. contributes to the region's economy and carbon sequestration potential. In this study, we used Virginia forest harvest maps to identify individual patches (stands) of pine forest which had each gone through a full harvest life cycle (rotation). With unique managed pine stands identified, we used satellite imagery to estimate growth of canopy leaf area over time within each stand, using a metric called leaf area index (LAI). We identified 13,140 separate stands, each with up to 28 years of available data. We took the first full-state census of areas of managed pines in Virginia, and their leaf area development. We acquired one LAI measurement from February of each year, for each stand in Virginia. Using February LAI for each of our stands, we found that an average stand in VA has a maximum winter LAI of 2.02 (meaning an approximate maximum summer LAI of 4.04), and that stands generally reached their peak LAI after around 14 years of growth. It is recommended, in VA, that a landowner fertilize their stand in the middle of a harvest rotation if summer peak LAI is under 3.5, at stand closure. We found that at ten years of stand age, 45.8% of stands were estimated to reach above this threshold. Since this study's dataset is the most comprehensive LAI dataset for managed pines in VA, it may be used to improve management outcomes as well as understand pine productivity for land surface modeling purposes.

Acknowledgements

I would like to acknowledge my advisor, Dr. R. Quinn Thomas, for unwavering support through many challenges, as well as a firm commitment to student development. I acknowledge my committee members, Dr. Randolph Wynne and Dr. Valerie Thomas for support, advice, and feedback throughout the degree process. I would like to thank the Ecosystem Dynamics and Forecasting Lab for providing unceasing feedback and a source of community and support. I would also like to thank Jobriath Kauffman for providing map materials and data, as well as advice on usage and other useful metadata. I must also thank the Forest Resources and Environmental Conservation community, both graduate students and staff, for valuable interactions, conversation, and support along the way. Lastly, I gratefully acknowledge the National Aeronautics and Space Administration for funding under grant NNX17AI09G.

Table of Contents

List of Figures

List of Tables

1. Introduction

1.1. Leaf Area Index Applications

Leaf area index (LAI), a metric describing the area of leaves in a canopy above a specified area of ground, is an important control on the amount of carbon (C) absorbed by terrestrial vegetation. Characterizations of spatial and temporal patterns of LAI can improve predictions of terrestrial primary production by serving as model inputs (Robinson et al., 2018; Running et al. 2004) and for evaluating model predictions (Lucht et al., 2002; Piao et al., 2006). Quantifying LAI dynamics of large regions, along with the spatial variation in metrics of LAI recovery post disturbance (such as the rate of change or maximum LAI), can provide benchmarks for models that predict LAI and help identify where limitations to productivity and carbon storage occur. In managed stands, LAI metrics have been used for management purposes as indicators of nutrient limitation in the system (Osem and O'Hara, 2016; Fox et al., 2007; Rubilar et al., 2018). For example, it is recommended that if, at stand closure, peak summer LAI in a pine stand falls below 3.5, that the site be fertilized in order to increase LAI (Vose and Allen, 1988; Fox et al., 2011). We will use this productivity threshold later in the paper, in order to put our findings in perspective.

1.2. Relevant Remote Sensing Methods

While ground-based loblolly pine LAI measurements have been applied in specific locations (Hennessey et al., 2004; Liu et al., 2018), it is logistically impractical to develop large-scale LAI maps based on these measurements. Therefore, it is necessary to focus on estimates that are derived from remote sensing. Global and spatially gridded estimation of LAI has been possible for some time now; this has been enabled by the development of moderate resolution earth

observation satellite data products by NASA and the USGS (Justice et al., 2002; Myneni et al., 2002). Advanced Very High Resolution Radiometer (AVHRR) LAI products have been available from 1981 to present, while MODIS LAI products have been available from 2001 until present. The resolution of these products ranges from AVHRR's 0.05 arc degrees to MODIS's 250 m^2. While these resolutions are adequate for many regional to globe scale studies, they are lacking in regions with high spatial heterogeneity of LAI, such as is the case in the southeastern U.S., where stand-scale ownership and forest management are common.

The Landsat land monitoring satellite series provides a long-term, 30m resolution, dataset of surface reflectance. This is especially useful for time series and change detection studies requiring dense stacks of images with high quality registration and calibration properties, designed to allow image timeseries inter-comparison. Landsat data allow sufficient spatiotemporal resolution to capture LAI responses to harvest events at the landscape scale, with month-by-month coverage. Therefore, Landsat data is ideal for the purposes of capturing spatial and temporal variation in regions such as the Southeastern U.S. While LAI products from MODIS have been operationalized for over a decade, LAI products based on Landsat are not yet widely available. Recently, Blinn et al. (2019) developed a linear model relating Landsat surface reflectance to LAI in managed loblolly pine plantations.

1.3. Loblolly Pine Management in the Southeast

Applying the recently developed Landsat-LAI model regionally has the potential to improve our understanding of LAI dynamics in managed pine ecosystems in the southeastern U.S. Understanding loblolly pine LAI in this region is especially important, as the southeast accounts for ~60% of timber production of the U.S.A, and pine plantations cause the southeast to be a

globally significant timber resource (Prestemon & Abt., 2002). Over the southeastern U.S., pine plantation dynamics are those of patchy, fine-grained, and fast-growing silvicultural systems with short rotation times (Hansen et al., 2013). This is partially due to intensive silvicultural prescriptions developed throughout the early 2000's, creating a framework in which intensively-managed stands output several times the timber yields of unmanaged stands (Allen, Fox, & Campbell., 2005; Fox et al., 2007; Rubilar et al., 2018; Albaugh et al., 2002). Southeastern forests are almost exclusively privately owned and managed, leading to the application of diverse management regimes (Prestemon & Abt, 2002). Pine plantation canopy area is likely to reflect the patchiness of management, and leafy canopy area is one of the main regulators of yearly increment growth and carbon sequestration (Allen, Fox, & Campbell., 2005; Fox, Allen, & Albaugh, 2007; Osem & O'Hara, 2016). While these characteristics make loblolly pine leaf area dynamics an important component in a production context as well as the context of land-atmosphere carbon exchange (Sellers et al., 1997; Bonan, 1990), there are no studies characterizing the landscape-scale spatiotemporal dynamics of LAI in pine plantation ecosystems across the southeastern U.S. This study focuses on a sub-region, the state of Virginia, within the southeast due to the availability of reliable management and disturbance maps in state for a significant portion of time within the acquisition timeframe of the Landsat archive. In the future, methods employed in this study could be used throughout the rest of the southeastern U.S.

1.4. Study Goals

Here we characterize the spatiotemporal patterns in pine plantation LAI across VA, in order to evaluate the rate of LAI regeneration post-stand establishment, and to examine spatial patterns of LAI at stand closure. First, we identified loblolly pine plantations in the state, and estimated

timeseries of LAI estimates from Landsat data using an empirical model. We then examined LAI dynamics from the time of an initial stand-clearing disturbance to the estimated time of a following clearcut, taking data on maximum winter LAI, and the time at which stands reached this maximum. Second, we evaluated patterns in LAI at ten years of stand growth (after the stand has been cleared). This study is the first to provide regional scale evaluation of stand-scale LAI dynamics while also highlighting areas within the region where management has potential to result in the greatest increase productivity.

2. Methods

2.1. Overview

We used remotely sensed products to identify stands that had gone through an entire harvest rotation. This allowed us to characterize LAI development, after stand-clearing disturbance, within pine stands throughout the study region. To develop metrics quantifying the temporal dynamics of LAI, we calculated three metrics: peak LAI, the year at which LAI reached its peak within the stand lifetime, and the LAI at age 10.

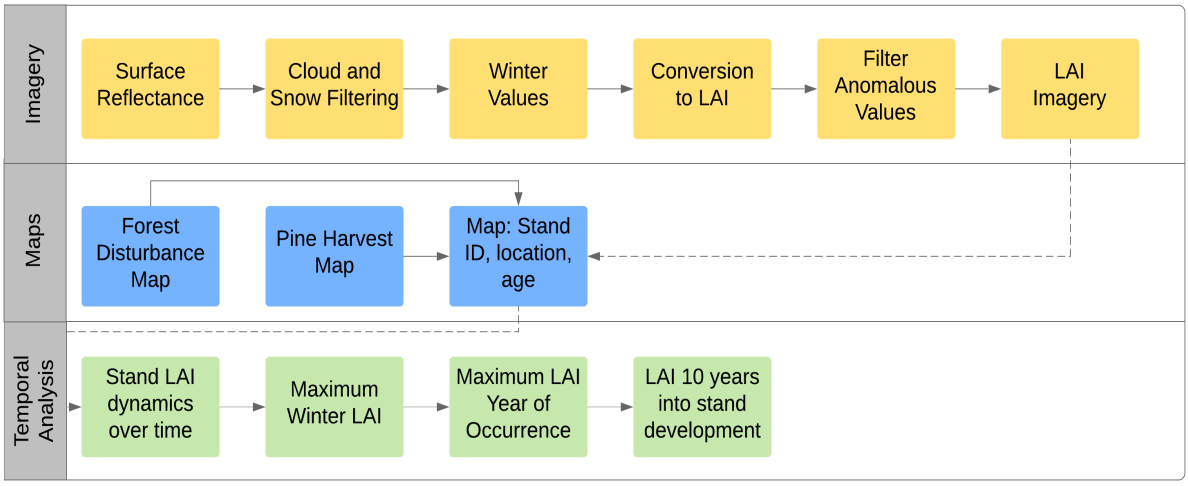

Figure 1. Workflow of estimation and analysis of leaf area index (LAI) for managed pine stands in Virginia

2.2. Study Location

Our study area was the state of Virginia (VA). We focused on this state because 1) it is a microcosm of the management style of the southeastern U.S., privately-owned loblolly pine plantations are common in Virginia and across the southeastern U.S (Prestemon and Abt, 2002), and 2) there are two data sources available for mapping disturbance: a map of stand-clearing disturbances in forests and the year of their occurrence (1984-2011) (Kauffman et al., 2016) and a map of clearcuts occurring in pine stands (2014-2017) (Thomas et al., 2019). Additionally, a

model used to generate a Landsat LAI data product for pine stands, was developed and evaluated for plots within Virginia (Blinn et al. 2019).

We extracted Landsat reflectance data throughout most of VA, with most pixels being located within the Piedmont and Coastal Plain physiographic regions, where managed pine plantations are most commonly found. Overall, the study area has a subtropical climate with variable precipitation and growing season over an east-west gradient, due to mountainous terrain in the western part of the state.

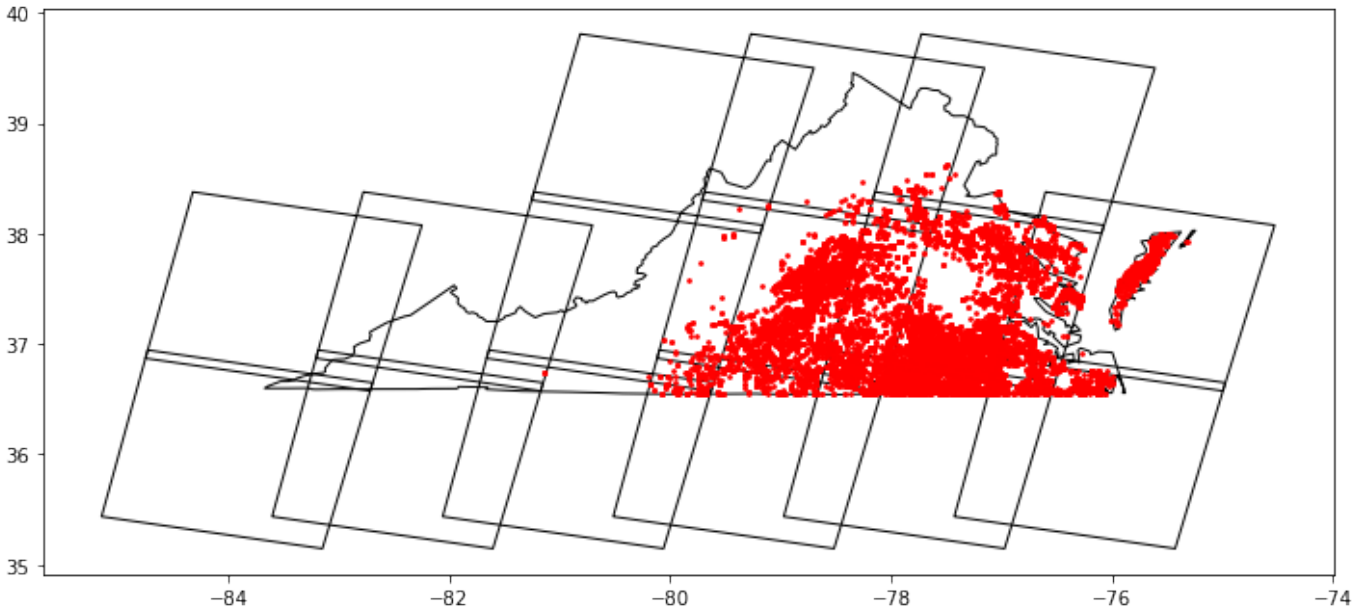

Figure 2. Study area: The State of VA, and all intersecting WRS-2 (Worldwide Reference System 2) path-rows.

2.3. Identifying pine stands

Our analysis focused on analyzing the LAI dynamics of all pine stands that were harvested in the 2014 – 2017 time period. To identify these stands, we first used a raster data product at the 15m scale, that classified pixels as either pine or non-pine. Within the larger pine classification, pixels were identified as either having been clearcut, thinned, or persistent through the years 2014 - 2017 (the acquisition timeframe) (Thomas et al., 2019). To generate the data product, Thomas et

al. applied a classification algorithm to timeseries Landsat data, and manually georeferenced training/test data from a database of water quality best management practices inspections throughout VA, from the Virginia Department of Forestry's Integrated Forest Resource Information System (http://www.dof.virginia.gov/gis/ifris.htm). Thomas et al. supplemented the georeferenced management data by adding originally created points at which pines persisted without management throughout the study period. Thomas et al. used NLCD and other supplementary data to create a base forest class, on which the further management classifications were implemented. To determine the year that each pixel was established, we used a one-band raster map (30m scale), based on the Vegetation Change Tracker (Kauffman and Prisley, 2016) that classified pixels as either stand-clearing disturbances, non-stand-clearing disturbances, persisting forest, persisting non-forest, or water during the 1984 – 2011 period, with dates of disturbance encoded in each pixel's band digital number (Kauffman and Prisley, 2016). We estimate the age of each pixel harvested in the 2014-2017 period by identifying the year of previous stand-clearing disturbance and subtracting that year from the harvest year. Since the map of harvests in the 2014-2017 is a three-year window, there was uncertainty in the estimated age that we explore in the discussion section. We assumed that pixels were not harvested, planted, and harvested again in the period when the disturbance map ends (2011) and the harvest map (2014).

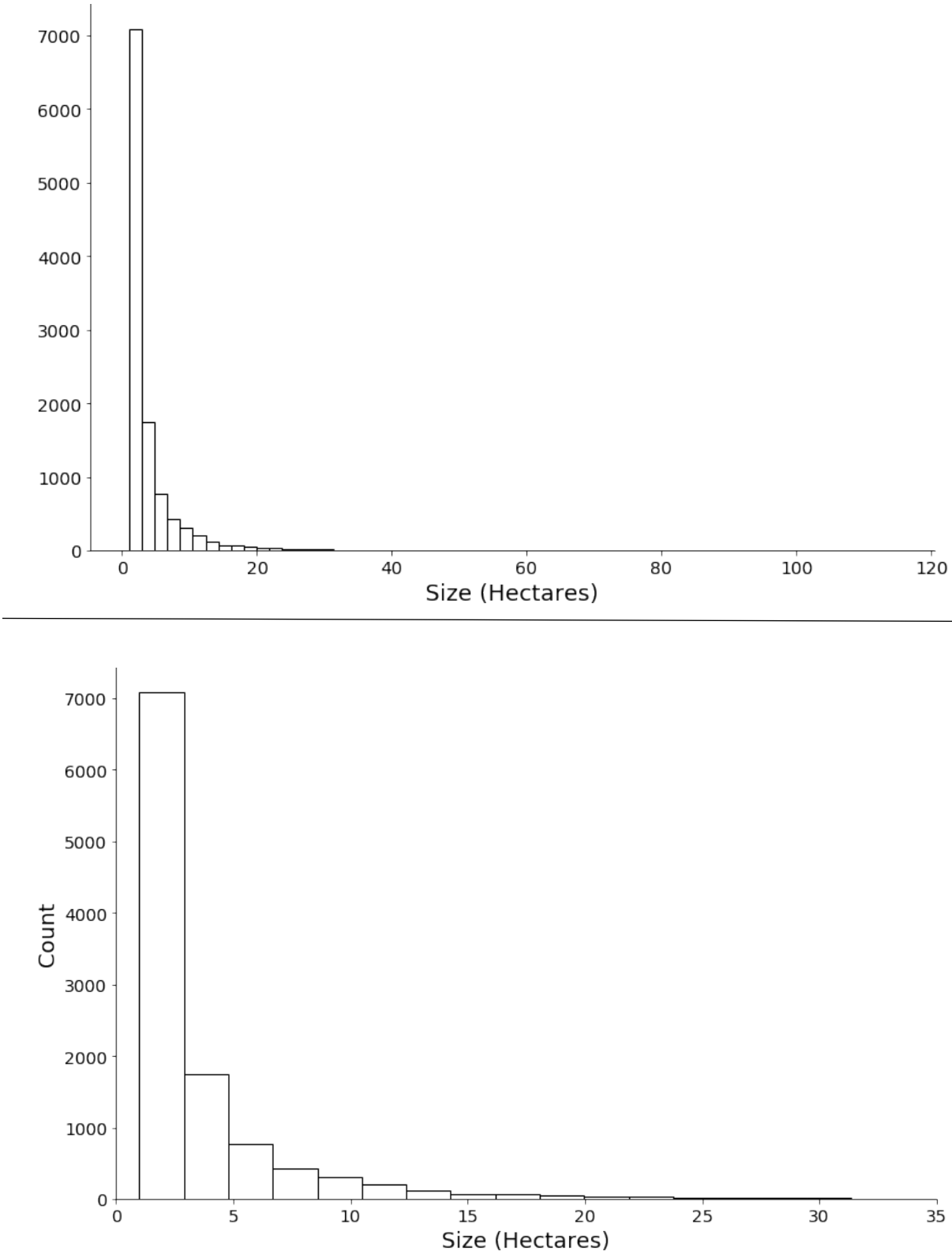

Figure 3. Stand size across VA, for stands detected in the context of the study

To create map of stands, we used pixels that met the following criteria: 1) they were pine and clearcut between 2014-2017 and 2) they had been previously harvested in the 1984 – 2011 time window. First, we defined this area as a raster intersection with the above conditions, and then converted it to a vector feature class. Second, we performed a 5m inward buffer for this feature class, in order to reduce the likelihood of slight mis-registrations causing overlaps of the feature class and non-relevant pixels. Third, we modified the feature class in such a way that it contained only single, geographically disparate, features with separate IDs (i.e., a stand). Fourth, we filtered the feature class so that it was provided an area threshold of a 3 x 3 square of pixels, in order to remove data from stands that were likely to be stand fragments, and to minimize data gathered from mis-classified single pixels. Lastly, we limited our scope to identified stands that were one hectare or more in area, in the hopes of removing noisy stand fragments.

2.4. Landsat Data

To generate a Landsat-derived LAI data product for each pine stand, we acquired Landsat 5 TM, Landsat 7 ETM+, and Landsat 8 OLI surface reflectance image collections (Masek et. al., 2006), using the Google Earth Engine (GEE) code editor for all available dates from the beginning of the disturbance map timeframe (1984) up to the beginning of the VDOF management dataset timeframe (2014). We used USGS Tier 1 Surface Reflectance data because of the atmospheric corrections and feature masking applied within the pre-processing of the data product. The masking includes a quality assurance (QA) band, giving pixel-specific information on clouds, cloud shadows, snow, and water. Surface reflectance pre-processing by the USGS involves the use of LEDAPS for atmospheric corrections, and CFMASK for the purpose of creating the QA band for each pixel. They are well-established algorithms, and greatly decrease pre-processing time for the image end user. The image collections of Landsat Surface Reflectance were masked

using a pixel-by-pixel application of the quality assurance bitmask for snow, clouds, and cloud shadows (annotated scripts provided for further detail on bitmask application). We selected red and near-infrared bands from these images for further processing ("Red" designation is equivalent to 0.63-0.69nm in Landsat 5 TM, 0.63-0.69nm in Landsat 7 ETM+, and 0.64-0.67 in Landsat 8 OLI. "Near Infra-red" designation is 0.85-0.88nm in Landsat 8 OLI, 0.77-0.90nm in Landsat 7 ETM+, and 0.76-0.90nm in Landsat 5 TM). These data products also were best-related to ground surface-measured LAI in the investigation by Blinn et al. (2019).

Table 1: Data Sources used in study

Map type	Map format	Spatial resolution	Description
Virginia Management Map	Raster	15m	A map of pine management across VA
Virginia Forest Disturbance Map	Raster	30m	A map of forest disturbances and the year at which they occur within VA
Landsat 5 TM	Raster	30m	Multi-band image time-series
Landsat 7 ETM+	Raster	30m	Multi-band image time-series
Landsat 8 OLI	Raster	30m	Multi-band image time-series

2.5. Estimation of LAI

We calculated LAI from simple ratio index using the linear model reported in Blinn et al. (2019) for all Landsat image acquisitions intersecting with stands in our dataset. Blinn et al. (2019) showed that, from surface reflectance datasets, simple ratio index (SR) resulted in the best fit

between a satellite index metric and observed LAI. We calculated SR for all images in the study area, over the timeframe of the study based on equation 1,

$$SR = \frac{NIR}{R} \quad \text{Equation 1}$$

where NIR is near infra-red reflectance and R is red reflectance. This is related to the health and vigor of a canopy (Zheng & Moskal, 2009; Slaton et al., 2001). Red light is used by the leaf's chloroplasts in order to perform photosynthesis, and its reflectance values are negatively related to plant and leaf health (Zheng & Moskal, 2009). Near infra-red-light reflectance is positively related to leaf vigor, and leaves with higher structural integrity and water content tend to reflect higher levels of NIR. Therefore, SR index increases with increasing canopy vigor, when SR is being derived from a forested pixel. We estimated LAI from SR using the linear model in Figure 3 of Blinn et al. (2019).

$$LAI = SR * 0.3329155 - 0.00212 \quad \text{Equation 2}$$

We extracted the data, from Google Earth Engine, into long-form tables, containing each polygon's ID number, area, and LAI timeseries. After the extraction of LAI timeseries for all of the pixels throughout study locations, we further filtered LAI based on the presence of outliers that were not considered biologically feasible. These outlying points may have existed for a number of reasons, including clouds, cloud shadows, radiometric or geometric mis-calibrations, or other reasons unaccounted for. However, they had a high likelihood of being artefacts by unknown cause, due to the fact that these LAI values have never been measured on the ground,

even at the most productive times of the year. Specifically, we defined an unrealistic value as a negative LAI, and LAI that was higher than 10 units (most LAI measurements for Loblolly Pine do not exceed 6 units at peak season (Landsberg et al., 1999; Albaugh et al., 1996).

Our analysis focused on the maximum LAI in the month of February, as an estimate of the winter minimum LAI for each year in the stand rotation. We focus on the February maximum because 1) using winter LAI values reduces the influence of non-pine (deciduous) species and 2) using the maximum of a winter month rather than the minimum of the entire winter removes the noise associated with low values of SR (therefore LAI) caused by snow and ice. Finally, for each stand we determined the LAI at age 10 as a metric of stand productivity. This was done in order to represent, spatially, an approximation of LAI near the time at which a stand's LAI is presumed to peak, and before the time at which most stands are thinned.

2.6. Analysis

We performed the following analyses:

1) We first calculated the mean and standard deviation at each age between 1 and 30 for all stands in the dataset.
2) We examined rotation ages for each stand.
3) We calculated the maximum winter LAI in each stand, and the age (in years) at which the maximum was reached. This analysis was only conducted for timeseries that had rotation lengths of over 20 years. This ensured that maximum values were not artefacts of the highest value before a premature cut, but rather representative of a value describing the highest that the stand had potential to grow to. As an example, a stand that is twenty years of age will most likely be described by an initial clearing,

possible pre-preparation/fertilization, and then a thinning around twelve to seventeen years of age. This makes a twenty-year old stand much more likely to contain a full spectrum of possible LAI values within its rotation, rather than a stand that may not have reached a meaningful peak value.

4) We examined the spatial distribution of this maximum winter LAI, across the state.

3. Results

3.1. General Pine Stand Information

In total we identified 13,140 stands across the state of Virginia with ages that ranged from 0 to 31 at the time of harvest (Figure 3). Most stands were harvested after age 22 (50th percentile). The 25th quantile of the age range was 14, and the 75th quantile of the age range was 22. The majority of stands were located in Franklin, Brunswick, and Virginia Beach counties. Managed pine stands in our study made up 0.28% of the area of the state, with a total area of 286.098km^2.

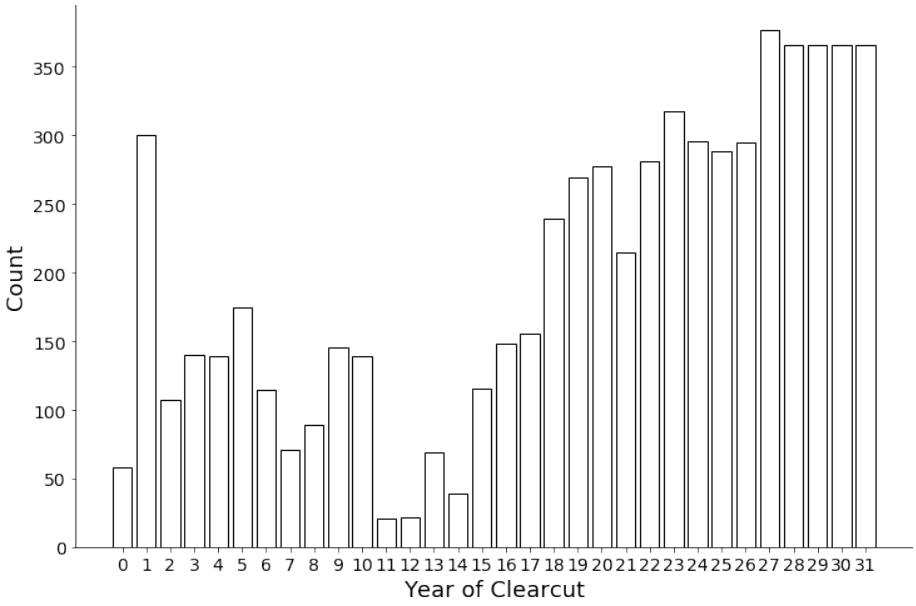

Figure 4. Harvest age for all stands in the State of VA. Stands were filtered using a 9*9 pixel area spatial threshold. For all stands, there is 3-year possible error (see methods).

3.2. Peak Leaf Area Index

On average, the stand-level winter LAI peaked at 17.24 years of age (Figure 6), with a standard error of 0.107. At the individual stand-scale, the average maximum winter LAI was 1.98 with the 95th percentile of the data ranging from 2.62 to 5.45.

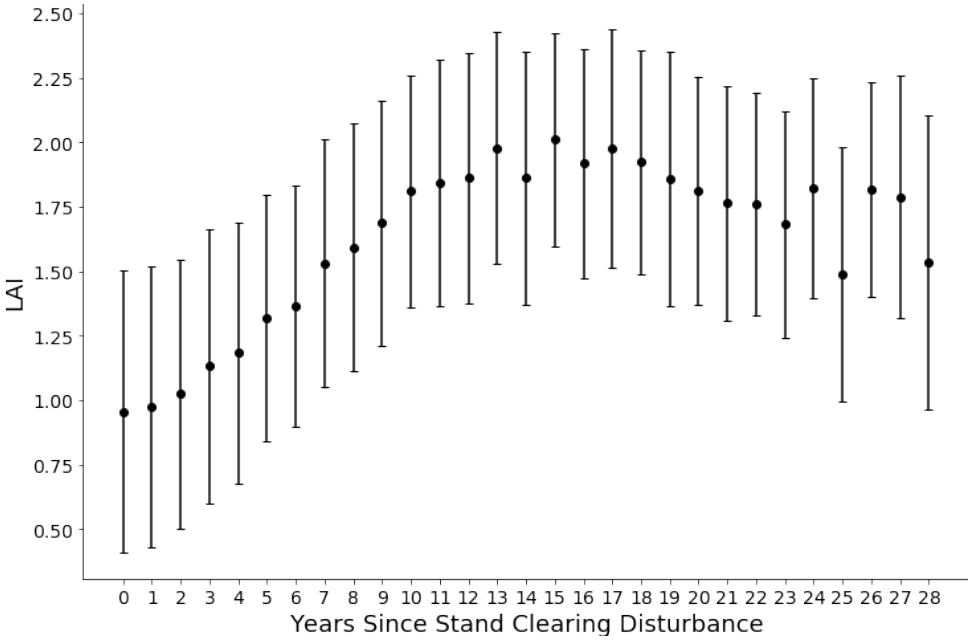

Figure 6. Mean and standard deviation LAI values through all stands in the study region, over time. Each stand's yearly LAI is equivalent to yearly February maximum (see methods).

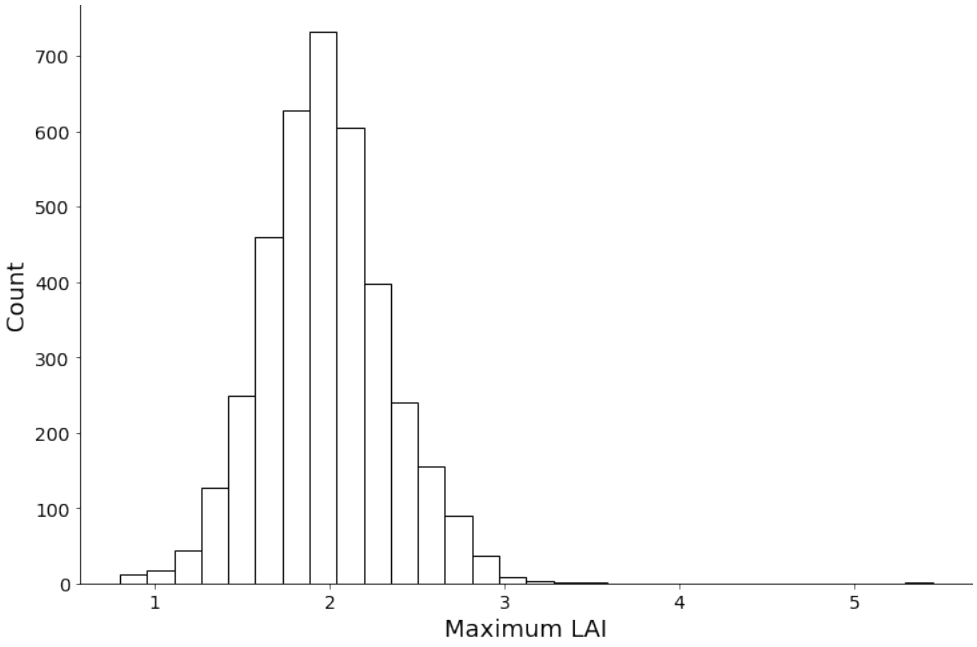

Figure 5. Maximum winter LAI for all years within each stand's rotation. The data shown only include stands that were clear-cut at least 20 years after their inital stand-clearing disturbance.

3.3. LAI Ten Years Post-Disturbance

At ten years after initial stand-clearing disturbance, 45.8% of stands' LAI values were over the canopy closure threshold from the FPC.

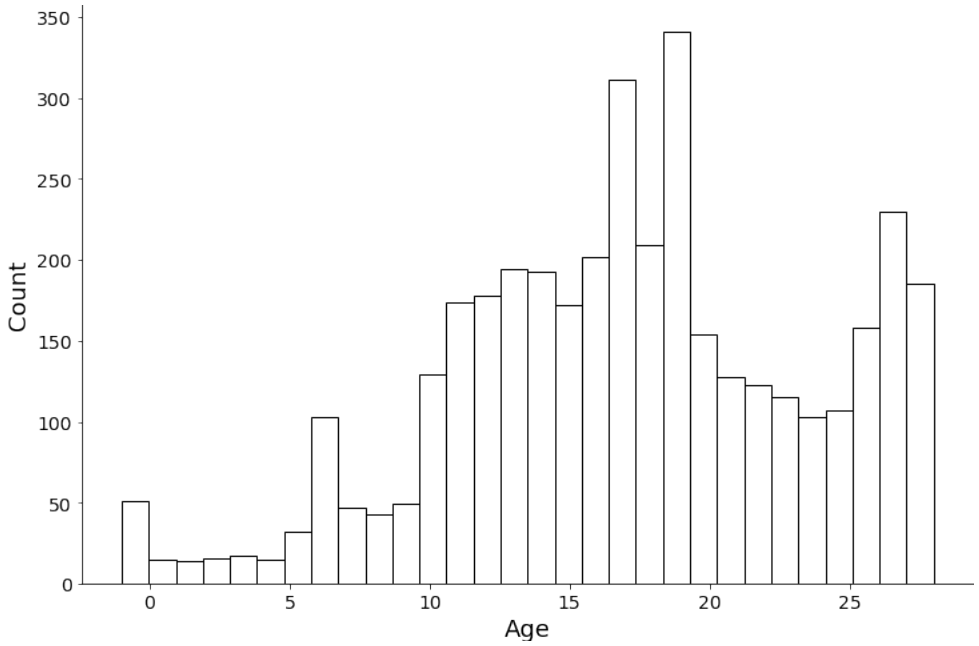

Figure 7. The age that LAI reached its maximum value within each stand across the study region. The data shown only include stands if clear-cutting occurred at least twenty years after the initial stand clearing disturbance.

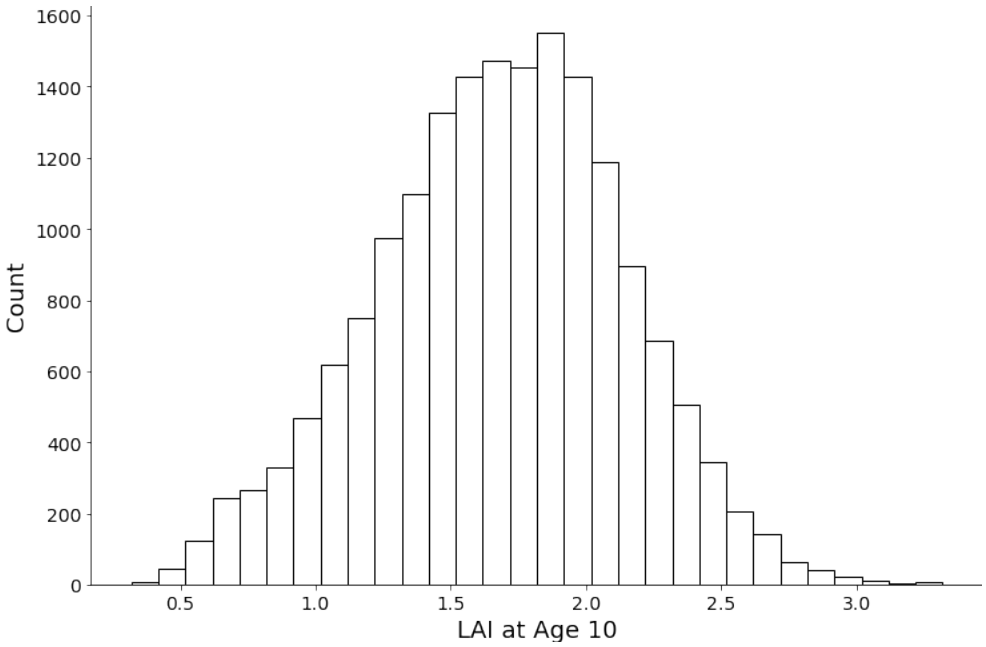

Figure 8. Leaf area index at age 10: for all stands in study area

4. Discussion

Random variation in LAI, remote-sensing noise, management, and environmental variables must drive differences between stands to different degrees. Environmental factors that can influence productivity include temperature, soil moisture, vapor pressure deficit, and soil fertility (Landsberg and Waring, 1997). While large scale climate variables such as temperature and precipitation are relatively similar across VA (Young et al., 2017; PRISM, 2016), further study could reveal precipitation and temperature as partial drivers of productivity within the scale of the study region. Topography and soils vary more throughout the state (USDA NRCS), and may be more interesting for further study as drivers of variation. Management factors include fertilization, site preparation, and mid-rotation vegetation control among other management techniques, and have

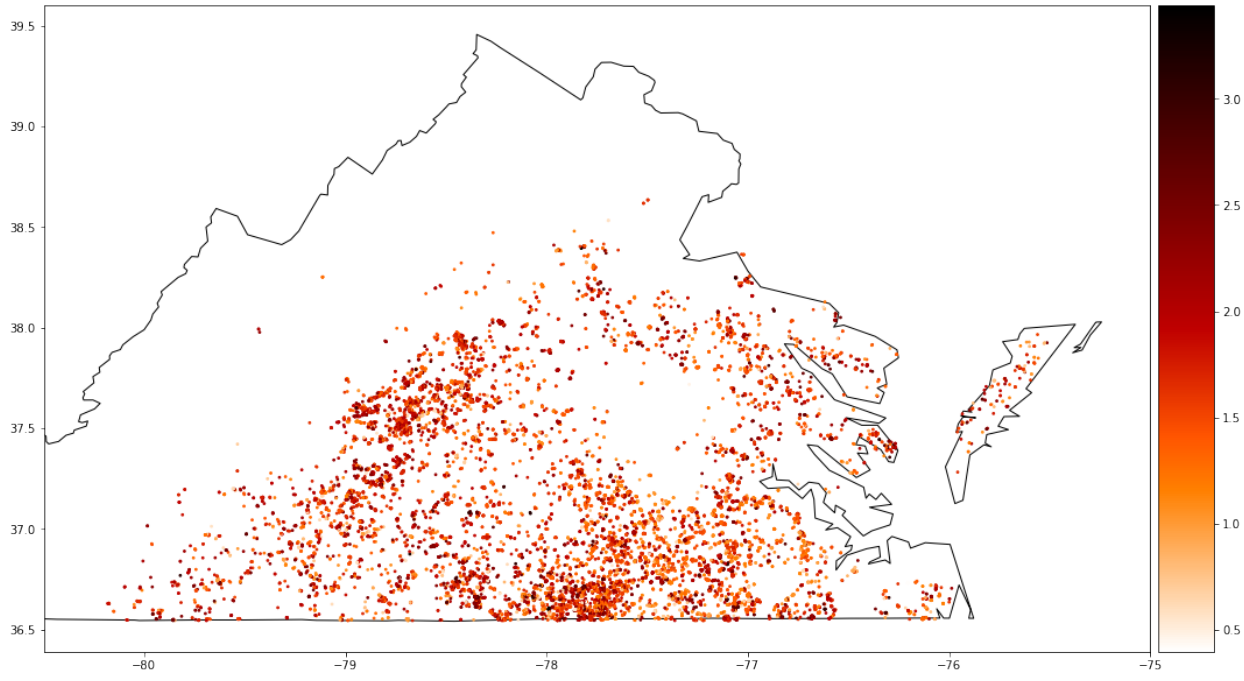

Figure 9. LAI at age 10

been shown to increase productivity with the correct implementation (Hennessey et al., 2004; Blazier et al., 2017; Osem and O'Hara, 2016; Albaugh et al., 2003; Allen, Fox and Campbell, 2005; Rubilar et al., 2018; Fox, Allen and Albaugh 2007). Management and environmental factors are the most likely drivers of LAI capacity and relative limitation, and further study is required to attribute management versus environmental causes over the state and region.

We found that the average maximum winter LAI is around 2. This corresponds to a summer pine LAI of around 4, roughly double its winter value, based on the work of Sampson et al. (2003). This approximate summer value aligns roughly with findings by Peduzzi et al. (2012) and Blinn et al. (2018). It should be noted that winter LAI for a site may be a better predictor of summer pine LAI than actual summer site LAI, due to the presence of competing deciduous vegetation. This finding reinforces information provided by past studies on loblolly pine, and can be used to better understand this specific plant type in a modeling context, eventually scaled across the larger southeastern region.

An average stand's LAI timeseries reaches a peak point at around 14 years of growth. A peak in LAI at this age is most likely the result of stand closure, followed by either within-stand light use competition, or thinning by stand managers; the timing of closure depends upon rate of leaf area development and spacing of stands, but can fall anywhere between 6-12 years (Campbell et al., 2015; Campbell et al., 2013; Radtke et al., 1999), however, Gonzalez-Benecke et al. (2014), in *Pinus elliottii* stands, estimated age of canopy closure to be 5. Thinning of stands also depends upon management goals, spacing, and other external factors, and is usually implemented around 7 - 14 years (Blazier et al., 2015; Blazier et al., 2017). The dip in LAI following the peak points to either stand competition, resulting from crown closure and sunlight limitation, or to thinning, intended to release stands from this crown closure and produce

straighter, taller and more merchantable stems. There has been much previous work identifying thinnings in southern pine plantations, and thus future work could focus on differentiating the post-peak LAI dip in a thinning context and in a stand competition context. This peak supports the use of LAI at age 10 as a basis for LAI capacity and relative limitation; LAI values measured before the time of thinning are more likely to reflect actual LAI regeneration than to capture post-thinning values.

One important limitation of this study is a lack of precision in the exact year of the harvest due to using a map with a four-year possible time window in which harvests may occur. The management map assembled by Thomas et al. (2019) has this limitation, but is used because of its power in selecting between clearcuts and thins; a sacrifice in temporal precision gives us better outcomes in map accuracy. The four-year time window has implications for temporal results: maximum LAI metrics will be affected by this limitation because of the possibility of maximum LAI occurring after the end of available data in this study. However, LAI at age10 will not be affected by this study limitation, except to reduce data availability slightly. Further work may overcome this limitation by combining maps that specify thins with maps that specify the year of disturbance, such as Hansen et al. (2013), within the necessary time window.

In the results, many stands are marked as having been harvested as early as zero years of age. This is likely due to classification of stands, within the map of VA disturbances, as stand-clearing disturbances as opposed to non-stand-clearing disturbances. This is most probably the case, both because clear-cutting a stand before ~10 years of age is not an advisable strategy for harvest returns, and because the disturbance map created by Kauffman et al. (2016) relies on the vegetation change tracker, which is known to sometimes mis-identify thinning events as

clearcuts. While this points to a limitation for interpretation, the methods used in this paper can be used with novel datasets as they become available.

In developing a picture of LAI dynamics and productivity across VA, we gain a platform for multiple forms of further research. For example, there is potential in the area of extending the mapping of LAI capacity to other regions, and comparing relative limitation in stands in any region with the prerequisite mapping products for identification of management and disturbance dates. There is further potential in the area of attributing causality to the patterns found in relative limitation across HUC10 units. Lastly, further work could be done with this spatiotemporal dataset in regard to spatial modeling and terrestrial vegetation simulations. Overall, we see this study as a proof of concept for large scale analysis of pine LAI dynamics and spatial patterns in productivity, and a jumping off point for numerous other potential studies.

5. Conclusions

This study makes available a dataset of managed pine LAI, over time and spatially, for the state of VA. In Virginia, we found that pines which had gone through a full management rotation, on average, reached maximum LAI at age 17, with a value of 2. We found that 45.8% of stands, at age 10, were above the FPC fertilization threshold. This data brings to light novel information on pine stands in the state, and motivates further management-related questions related to increasing LAI at stand closure. The methodology for acquisition of this dataset is repeatable, and has potential as a useful asset for creating similar datasets for both managed pines and other plant types. Furthermore, this data has application to efforts in modeling the interactions of managed pines with the land surface and atmosphere in terrestrial ecosystem models.

References

Albaugh, T. J., Allen, H. L., Zutter, B. R., & Quicke, H. E. (2003). Vegetation control and fertilization in midrotation Pinus taeda stands in the southeastern United States. Annals of Forest Science, 60, 221–233. https://doi.org/10.1051/forest:2003054

Allen, H. L., Fox, T. R., & Campbell, R. G. (2005). What is ahead for intensive pine plantation silviculture in the South? Southern Journal of Applied Forestry, 29(2), 62–69. https://doi.org/10.1093/sjaf/29.2.62

Blinn, C. E., House, M. N., Wynne, R. H., Thomas, V. A., Fox, T. R., & Sumnall, M. (2019). Landsat 8 based leaf area index estimation in loblolly pine plantations. Forests, 10(3), 1–18. https://doi.org/10.3390/f10030222

Fox, T., Allen, H., & Albaugh, T. (2007). Tree nutrition and forest fertilization of pine plantations in the southern United States. Southern Journal of Applied Forestry, 31(1), 5–11. https://doi.org/10.1093/sjaf/31.3.129

Fox, T.R., Miller, B.W., Rubilar, R. Stape, J.L., Albaugh, T.J. 2011. Phosphorus Nutrition of Forest Plantations: The Role of Inorganic and Organic Phosphorus. in E.K. Bünemann et al. Phosphorus in Action: Biological Processes in Soil Phosphorus Cycling, Soil Biology, 26.

Hansen, M. C., Potapov, P. V, Moore, R., Hancher, M., Turubanova, S. a, Tyukavina, A., … Townshend, J. R. G. (2013). High-Resolution Global Maps of 21st-Century Forest Cover

Change. Science (New York, N.Y.), 850(November), 2011–2014. https://doi.org/10.1126/science.1244693

Hennessey, T. C., Dougherty, P. M., Lynch, T. B., Wittwer, R. F., & Lorenzi, E. M. (2004). Long-term growth and ecophysiological responses of a southeastern Oklahoma loblolly pine plantation to early rotation thinning. Forest Ecology and Management, 192(1), 97–116. https://doi.org/10.1016/j.foreco.2004.01.008

Jiménez-Gutiérrez, J. M., Valero, F., Jerez, S., & Montávez, J. P. (2019). Impacts of Green Vegetation Fraction Derivation Methods on Regional Climate Simulations. Atmosphere, 10(5), 281. https://doi.org/10.3390/atmos10050281

Justice, C. O., Townshend, J. R. G., Vermote, E. F., Masuoka, E., Wolfe, R. E., Saleous, N., … T, M. J. (2002). An overview of MODIS Land data processing and product status, 83, 3–15.

Kauffman, J. S., & Prisley, S. P. (2016). Automated estimation of forest stand age using vegetation change tracker and machine learning. Mathematical & Computational Forestry & Natural Resource Sciences, 8(1), 4–13. Retrieved from http://search.ebscohost.com/login.aspx?direct=true&db=asx&AN=117833076&site=eds-live

Kim, T. J., Wear, D. N., Coulston, J., & Li, R. (2018). Forest land use responses to wood product markets. Forest Policy and Economics, 93(May), 45–52. https://doi.org/10.1016/j.forpol.2018.05.012

Liu, X., Sun, G., Mitra, B., Noormets, A., Gavazzi, M. J., Domec, J. C., … McNulty, S. G. (2018). Drought and thinning have limited impacts on evapotranspiration in a managed pine plantation on the southeastern United States coastal plain. Agricultural and Forest Meteorology, 262(March), 14–23. https://doi.org/10.1016/j.agrformet.2018.06.025

Lucht, W., Prentice, I. C., Myneni, R. B., Sitch, S., Friedlingstein, P., Cramer, W., … Smith, B. (2002). Climatic control of the high-latitude vegetation greening trend and Pinatubo effect. Science, 296(5573), 1687–1689. https://doi.org/10.1126/science.1071828

Masek, J. G., Vermote, E. F., Saleous, N. E., Wolfe, R., Hall, F. G., Huemmrich, K. F., … Lim, T. (2006). A Landsat Surface Reflectance Dataset for North America, 1990-2000. IEEE Geoscience and Remote Sensing Letters, 3(1), 68–72. https://doi.org/10.1109/LGRS.2005.857030

Myneni, R., Hoffman, S., Knyazikhin, Y., Privette, J. L., Glassy, J., Tian, Y., … Running, S. W. (2002). Global products of vegetation leaf area and fraction absorbed PAR from one year of MODIS data. Remote Sensing of Environment, 83, 214–231.

Osem, Y., & O'Hara, K. (2016). An ecohydrological approach to managing dryland forests: Integration of leaf area metrics into assessment and management. Forestry, 89(4), 338–349. https://doi.org/10.1093/forestry/cpw021

Piao, S., Friedlingstein, P., Ciais, P., Zhou, L., & Chen, A. (2006). Effect of climate and CO2 changes on the greening of the Northern Hemisphere over the past two decades. Geophysical Research Letters, 33(23), 2–7. https://doi.org/10.1029/2006GL028205

Prestemon, J. P., & Abt, R. C. (2002). Chapter 13: Timber Products Supply and Demand. The Southern Forest Resource Assessment, 53, 299–325. Retrieved from https://www.fs.usda.gov/treesearch/pubs/42386

Robinson, N. P., Allred, B. W., Smith, W. K., Jones, M. O., Moreno, A., Erickson, T. A., Running, S. W. (2018a). Terrestrial primary production for the conterminous United States derived from Landsat 30 m and MODIS 250 m. Remote Sensing in Ecology and Conservation, 4(3), 264–280. https://doi.org/10.1002/rse2.74

Rubilar, R. A., Lee Allen, H., Fox, T. R., Cook, R. L., Albaugh, T. J., & Campoe, O. C. (2018). Advances in Silviculture of Intensively Managed Plantations. Forest Management, 4(1), 23–34. https://doi.org/10.1007/s40725-018-0072-9

Running, S. W., Nemani, R. R., Heinsch, F. A., Zhao, M., Reeves, M., & Hashmito, H. (2004). A Continuous Satellite-Derived Measure of Global Terrestrial Primary Production. BioScience, 54(6), 547. https://doi.org/10.1641/0006-3568(2004)054[0547:acsmog]2.0.co;2

National Cooperative Soil Survey. National Cooperative Soil Characterization Database. Available online. Accessed 12/12/2019.

Thomas, V.A., R.H. Wynne, R.Q. Thomas, C. Blinn, J. Kauffman, E. Brooks, P. Williams, W. McCurdy, M. House, L. Chini, R.B. Mei, D. Wear. 2019.- Regionally Specific Drivers of Land Use Transitions and Future Scenarios. NASA LCLUC 2019 Science Meeting, April 4-11, 2019, Rockville, MD.

Vose, J.M., Allen, H.L., 1998. Leaf Area, Stemwood Growth, and Nutrition Relationships in Loblolly Pine. Forest Science. 34(3), 547-563.

Zheng, G., & Moskal, L. M. (2009). Retrieving Leaf Area Index (LAI) Using Remote Sensing: Theories, Methods and Sensors. Sensors, 9(4), 2719–2745. https://doi.org/10.3390/s90402719

Appendix A: Google Earth Engine Code for LAI Timeseries Extraction

```
// Load in all imported data. The two maps are not publicly available at this time.
// One was obtained by contacting the author of an existing publication, and
// the other is in the process of publication in a scientific journal.
var Landsat8 = ee.ImageCollection("LANDSAT/LC08/C01/T1_SR"),
 Landsat5 = ee.ImageCollection("LANDSAT/LT05/C01/T1_SR"),
 Landsat7 = ee.ImageCollection("LANDSAT/LE07/C01/T1_SR"),
 huc10 = ee.FeatureCollection("USGS/WBD/2017/HUC10"),
 states = ee.FeatureCollection("TIGER/2018/States"),
 VA_Thins = ee.Image("users/cmwyatt5/Spring2019/VA_3class_newcodes_Project"),
 VA_Disturbance = ee.Image("users/cmwyatt5/Spring2019/Joby_Original_Map"),
 point = /* color: #d63000 */ee.Geometry.Point([-78.86020857961137, 37.20877477348371]);
// Load in Virginia boundaries
var VA = states.filter(ee.Filter.eq("STATEFP", "51"));
// Load in huc10 unit boundaries
var hucs = huc10.filterBounds(VA);
hucs = hucs.filter(ee.Filter.neq("huc10", "0301020205"));
// Define Area Threshold -- Equivalent to 9 pixels
var areaThreshold = (30 * 30) * 9;
// Define inward buffer magnitude
var howMuchBuff = -5;
////////////////////////////////////////// DEFINE FUNCTIONS ////////////////////////////////////////////////////////////
// mask landsat 5 and 7
function cloudMaskL457(image){
 var qa = image.select('pixel_qa');

 var cloudMed = qa.bitwiseAnd(1 << 5) // set qa bit to cloudy
 .and(qa.bitwiseAnd(1 << 7)) // get medium confidence cloud
 .or(qa.bitwiseAnd(1 << 3)) // or else cloud shadows
 .or(qa.bitwiseAnd(1 << 4));

 // var snow = qa.bitwiseAnd(1 << 4); // get snow bit

 var mask2 = image.mask().reduce(ee.Reducer.min());

 return image //mask out high confidence clouds
 .updateMask(cloudMed.not()) // mask out medium confidence clouds
 .updateMask(mask2); // mask out surrounding pixels
}
29
// mask lansdsat 8
function maskL8sr(image) {
 // Get the pixel QA band.
 var qa = image.select('pixel_qa');
 var cloud = qa.bitwiseAnd(1 << 5) // cloud flag set
```

```
 .and(qa.bitwiseAnd(1 << 7)); // or the cloud HIGH set

 var cirrus = qa.bitwiseAnd((1 << 9)) // cirrus flag set high
 .and(qa.bitwiseAnd(1 << 5)); // and cloud flag set

 var snow = qa.bitwiseAnd(1 << 4); // snow flag set

 var shadow = qa.bitwiseAnd(1 << 3); // cloud shadow flag set

 // Return the masked image
 return image.updateMask(cloud.not())
 .updateMask(cirrus.not())
 .updateMask(snow.not())
 .updateMask(shadow.not());
}
// These provide simple ratio index. Dividing near infra-red by red.
function simpleRatioL457(image){
 var ratio = image.expression(
 'NIR / RED ', {
 'NIR': image.select('B4'),
 'RED': image.select('B3')
 }).rename('simpleRatio');
 return image.addBands(ratio)
 .select('simpleRatio');
}
function simpleRatio8(image){
 var ratio = image.expression(
 'NIR / RED ', {
 'NIR': image.select('B5'),
 'RED': image.select('B4')
 }).rename('simpleRatio');
 return image.addBands(ratio)
 .select('simpleRatio');
}
// Leaf area index (LAI) from simple ratio (SR)
30
var LAIfmSR = function(image){
 var LAI = image.expression(
 "SR * 0.3329155 - 0.00212", {
 "SR": image.select("simpleRatio")
 }).rename("LAI");
 return image.addBands(LAI)
 .select("LAI");
};
//////////////////////////////////////////////////////////////////
//////////////////////////////////////////////////////////////////
```

```
//////////////////////////////////////////////////////////////
/////////////////////////////////////////////////// CREATE LAI IMAGE COLLECTION
//////////////////////////////////////////////////////////////
// # Filter Landsat5, 7, and 8 surface reflectance
// # using the cloud mask, the simple ratio function, and the LAI function.
// # This will give us a collection of one-band LAI images.
var Landsat5_LAI = Landsat7.map(cloudMaskL457).map(simpleRatioL457).map(LAIfmSR);
var Landsat7_LAI = Landsat5.map(cloudMaskL457).map(simpleRatioL457).map(LAIfmSR);
var Landsat8_LAI = Landsat8.map(maskL8sr).map(simpleRatio8).map(LAIfmSR);
// # The merged collection of all the LAI image stacks.
var collection = Landsat5_LAI.merge(Landsat7_LAI).merge(Landsat8_LAI)
.sort("system:time_start");
// # Filter to give only data from the winter months. December through February.
// # Then filter to make sure that data only comes from path-rows 16-34 and 15-34.
var winterCollection = collection.filter(ee.Filter.calendarRange(2,2,'month'))
.filterBounds(VA);
//////////////////////////////////////////////////////////////
//////////////////////////////////////////////////////////////
//////////////////////////////////////////////////////////////
////////////////////////////////////////// CREATE STUDY AREA MASK
//////////////////////////////////////////////////////////
// Mask thinning map for values corresponding to clearcut
var clr_Mask = VA_Thins.eq(2);
var clearcut = VA_Thins.updateMask(clr_Mask);
// Mask disturbance map for values corresponding to stand-clearing
31
var dist_Mask = VA_Disturbance.gt(13);
var dist_Mask2 = VA_Disturbance.lt(43);
var std_clr = VA_Disturbance.updateMask(dist_Mask).updateMask(dist_Mask2);
// Take the intersection of clearcut and stand-clear maps
var stdClr_and_clrCut = clearcut.and(std_clr);
// var finalClrCut = clearcut.updateMask(stdClr_and_clrCut);
// Use the intersection to mask the stand clearing disturbance map
var finalStdClr = std_clr.updateMask(stdClr_and_clrCut);
function pullHUC(huc){
 // {

 // Stage 1: The feature collection
 var vectorVersion = finalStdClr.reduceToVectors({
 scale: 10,
 geometryInNativeProjection: true,
 geometryType: "polygon",
 maxPixels: 5058413600,
 geometry: huc.geometry() // Define the limiting geometry
 });
```

```
 var buff = vectorVersion.geometry().buffer(howMuchBuff);
 var vectorCollection = ee.FeatureCollection(buff);
 var onlyPolys = vectorCollection.map(function(feat){
 feat = ee.Feature(feat);
 var geometries = feat.geometry().geometries(); // return a list of each geometry
 var extractPolys = ee.FeatureCollection(geometries.map(function(poly){
 poly = ee.Geometry.Polygon(ee.Geometry(poly).coordinates());
 return ee.Feature(poly);
 }));
 return extractPolys;
 }).flatten(); // Flatten because it's a collection of collections
 var polysWithArea = onlyPolys.map(function(feature){
 return feature
 .set("ID", feature.id())
 .set("area", feature.geometry().area());
 });
 var areaSubset = polysWithArea.filter(ee.Filter.gt("area", areaThreshold));

 // Get disturbance codes from the intersection raster, based on the subset of area.
 var disturbance_table = finalStdClr.reduceRegions({
 collection: areaSubset,
32
 reducer: ee.Reducer.mean()
 });
 // feature collection above
 //} // Disturbance Table

 // Create data table with LAI, and information from polygons
 var quad = winterCollection.map(function(image) {
 return image.reduceRegions({
 collection: disturbance_table,
 reducer: ee.Reducer.mean(),
 scale: 30
 }).filter(ee.Filter.neq('mean', null))
 .map(function(f) {
 return f.set('imageId', image.id());
 });
 }).flatten();

 return quad;
}
var pulledHUCS = hucs.map(pullHUC).flatten();
Export.table.toDrive({
 collection: pulledHUCS,
 description: "HUC10_LAI_Timeseries_HucCut",
 folder: "HUC10_LAI_Timeseries"
```

```
});
////////////////////////////////////////////////////////////////
////////////////
////////////////////////////////////////////////////////////////
```